



Adsorptive Remediation of Crude Oil Contaminated Marine Water Using Chemically and Thermally Modified Coconut (*Cocos nucifera*) Husks

Samuel E. Agarry^{1*}, Kigho M. Oghenejoboh², Ewomazino. O. Oghenejoboh², Chiedu N. Owabor³,
Oladipupo O. Ogunleye¹

¹ Biochemical and Bioenvironmental Engineering Laboratory, Department of Chemical Engineering, Ladoko Akintola University of Technology, P. M. B. 4000, Ogbomoso, NIGERIA.

² Biochemical and Bioenvironmental Engineering Laboratory, Department of Chemical Engineering, Delta State University, Abraka, P. M. B. 22, Oleh Campus, NIGERIA.

³ Department of Chemical Engineering, Federal University of Petroleum Resources, Effurun, NIGERIA

Received: 17/01/2020

Accepted: 04/04/2020

Published: 20/05/2020

Abstract

This study evaluated the potential of a chemically and thermally modified coconut husk as oil-spill sorbents in the remediation of crude oil contaminated marine water under varying physical factors of sorption time, initial oil concentration, temperature, sorbent dosage and oil weathering number of days. Coconut husk (CH) was chemically activated with zinc chloride and then pyrolyzed at a different combination of temperatures-retention times of 400 -800 °C and 30 – 60 minutes to produce un-activated and activated coconut husk-derived biochar (CHB and ACHB), while acetylated-coconut husk (ACCH) was produced using acetic anhydride. The results revealed that the sorption potential of coconut husk can be enhanced by chemical, thermal (pyrolysis) and chemo-thermal treatments (chemical/pyrolysis). The oil sorption capacities and oil removal efficiencies of raw CH, ACCH, CHB₈₀₀₋₆₀, and ACHB₈₀₀₋₆₀ were a function of the physical factors. The rate of oil sorption by raw CH, ACCH, and CHB₈₀₀₋₆₀ follows pseudo-second-order kinetics while that of ACHB₈₀₀₋₆₀ follows pseudo-first-order kinetics. The oil sorption by raw CH, ACCH, CHB₈₀₀₋₆₀ and ACHB₈₀₀₋₆₀ occurs via both surface and intraparticle diffusion mechanism. Freundlich isotherm best describe the oil sorption behaviour of ACCH, CHB₈₀₀₋₆₀, and ACHB₈₀₀₋₆₀, respectively, while Langmuir isotherm best describes the sorption of raw CH. The maximum monolayer sorption capacities were 12.11 g/g, 15.06 g/g, 16.10 g/g, and 16.84 g/g for the raw CH, ACCH, CHB₈₀₀₋₆₀ and ACHB₈₀₀₋₆₀, respectively, and hence the performance of the sorbents was in the following order: ACHB₈₀₀₋₆₀ > CHB₈₀₀₋₆₀ > ACCH > raw CH.

Keywords: Adsorptive remediation; Isotherms; Kinetics; Modified coconut husk; Oil spill

1 Introduction

Small and massive scale of oil spills occurs yearly on land, sea and marine water systems throughout the world as a result of human mistakes and carelessness, deliberate acts of pipeline vandalism, earthquakes, natural disaster [1], offshore drilling and production activities, crude oil transports by ships, cargos, vessels, tankers, rail and trucks, untreated oily waste disposal from petroleum refineries, factories and industrial facilities [2]. For the cleanup strategies of oil in the coastal or marine environment, several oil spill removal methods have been used, such as the use of solidifiers, dispersants and controlled in-situ burning, bioremediation, booms, skimmers and sorbent/adsorbent [3].

Adsorption technology has been observed to be one of the most effective method for oil spill removal or treatment. The sorbents that are used for oil spill removal are classified as

inorganic mineral, organic synthetic and organic vegetable [4-6]. Among the various commercial oil sorbents that have been deployed for oil spill removal, synthetic sorbent made up of polypropylene, polyethylene, and polyurethanes, and several cross-linked polymeric materials are the most commonly employed due to their good oleophilic and hydrophobic characteristics [6-9]. However, the major disadvantages of these sorbents are that they are not biodegradable [6, 8, 10], sometimes have low sorption capacity and are often expensive [6, 8, 11]. Therefore, there is a renewed attention and interest in the usage of natural sorbents as one of the most attractive options for oil spill remediation due to their low cost, eco- friendliness, effectiveness, low water pickup, high buoyancy, good reusability and high sorption capacity [12-13].

A wide variety of natural sorbents employed for oil spill remediation in water have been reported in the literature. These

Corresponding author: Samuel E. Agarry, Biochemical and Bioenvironmental Engineering Laboratory, Department of Chemical Engineering, Ladoko Akintola University of Technology, P. M. B. 4000, Ogbomoso, NIGERIA. E-mail: sam_agarry@yahoo.com.

include banana peels [6], modified pomelo peels [14], human hair [15], corncob [9], luffa fibre [16], rice husk [5], coconut coir [17], barley straw [18], and sugarcane bagasse [4]. However, the major draw-back of these agricultural plant-derived sorbents when present in saturated oil-water environments is their tendency to adsorb both water as well as oil, causing them to sink [17] as a result of low hydrophobicity and poor buoyancy when compared to synthetic sorbents such as poly-propylene [9, 11]. That is, when agricultural plant-derived sorbents are applied to saturated oil-water environments, water sorption is preferentially favoured over oil sorption because of the typical hydrophilic (due to abundant associated hydroxyl functional groups in the cellulose, hemicelluloses and lignin) nature of the sorbent [17]. Hydrophobicity or oleophilicity is one of the major advantages of sorbent characteristics that influences oil sorption effectiveness in the presence of water [19]. The sorbents effectiveness in saturated oil-water environments would be enhanced when the amount of hydroxyl functional group present is reduced (i.e. hydrophilicity is reduced) and hydrophobicity is increased [19]. The amount of hydroxyl functional group of these sorbents can be reduced by chemical modification, such as acetylation, acylation, acrylation, benzylation, cyanoethylation, and methylation [20] and as well as by thermal modification (pyrolysis) in the production of biochar. This chemical reactions involves the replacement of the hydroxyl functional group in the cellulose, hemicelluloses, and lignin present at the polymeric backbone with more hydrophobic groups [17].

The use of biochar as a potential eco-friendly adsorbent for wastewater and water purification has of recent received increasing attention [21-23]. Biochar can be produced from a myriad of discarded organic and biologically-based materials, including agricultural by-products or wastes. Several biochar derived from pyrolysis of agricultural wastes have been explored for a variety of applications including their adsorption potential for heavy metal removal from contaminated water [21-23], while very few works involving their use as oil adsorbents (such as rice husk biochar, corncob biochar, cornstalk biochar) in the removal of oil have been reported in the literatures [24-27]. Thus, a study for the implementation of biochar as sorbent for oil sorption needs to be fully developed. According to Camilli et al. [28] and Reddy et al. [29] there is the need to develop an effective, fast and cheap methods to minimize or mitigate the negative consequences of oil spill. However, report or information on the use of thermally and chemically modified coconut husk (a commonly available low-cost fibrous layer of lignocellulosic waste material found outside the coconut shell) as oil sorbents is seldom scarce.

Since coconut husk tends to also adsorb water, its oil sorption capacity may be reduced. Thus, acetylation reaction and pyrolysis are introduced to increase the hydrophobicity of the husks. Therefore, the major focus of this work are to (1) chemo-thermally modify the coconut husk through chemical activation using zinc chloride as agent and pyrolysis to produce activated coconut husk-biochar, (2) chemically modify the coconut husk through acetylation to produce acetylated-coconut husk and (3) evaluate and compare the potentials and efficiencies of the raw coconut husks and the resulting modified coconut husks (coconut husk derived-biochar, activated coconut husk-derived biochar and acetylated-coconut husk) as oil sorbents in the remediation of crude oil contaminated marine water under varying conditions of sorption time, temperature, oil concentration, oil weathering and sorbent dosage. Attempts have also been made to study the

engineering aspects of the removal or sorption mechanism such as kinetics and equilibrium of the crude oil sorption onto the sorbents.

2 Materials and Methods

Simulated marine water was used for the remediation studies. Chemicals and reagents used for the studies were of analytical grade (Sigma-Aldrich, Germany). De-ionized water was made used of throughout the experiments. Raw coconut husks (CH) used for the studies were obtained from a small scale coconut chips factory.

2.1 Preparation of simulated marine water

The preparation of simulated marine water for this study was carried out according to the recipe of Kester et al. [30] and Nwadiogbu et al. [9]. Ten (10) litres of de-ionized water was measured into a 20-L plastic container and the following quantities of salts (chemicals) were weighed and added into it as follows: Sodium chloride (NaCl) 23.926 g, Sodium sulphate (NaSO_4) 4.008 g, Potassium chloride (KCl) 0.667 g, Sodium bicarbonate (NaHCO_3) 0.196 g, Potassium bromide (KBr) 0.098 g and Boric acid (H_3BO_3) 0.026 g. For thorough mixing, the mixture was then stirred vigorously with a stirring rod.

2.2 Preparation of chemically modified coconut husk (acetylated coconut husks)

The raw coconut husks (CH) were chemically modified by acetylation reaction. Raw CH were sorted out so that sand impurities can be removed. The sorted coconut husks were sun-dried and then comminuted into samples of uniform size. Prior to acetylation of the raw CH, the influence of the CH fibre on acetylation was reduced. This was done by weighing 20 g of the sieved comminuted samples of the CH and then extracted in a Soxhlet apparatus for 5 h with a mixture of n-hexane and acetone (1:4, v/v). The residue CH were then oven-dried at 60 °C for 16 h. The extracted content was calculated as a percentage of the oven-dried coconut husks. The oven-dried CH were then acetylated using the method of Sun et al. [20]. This method of acetylation was carried out in a solvent-free system using acetic anhydride in the presence of N-bromosuccinimide (NBS) as catalyst. Ten (10) grams of dried-extracted CH were put into a round-bottom flask and thereafter 200 mL of acetic anhydride as well as 1% NBS catalyst were added. The round-bottom flask was fitted to a condenser and then placed in an oil bath that is on top of a thermostat- controlled heating device set at a temperature of 100 °C and the reaction was left for 1 h.

Thereafter, the round-bottom flask was taken out from the oil bath and the hot reagent was decanted. The CH were then washed thoroughly with acetone and ethanol. This was done to remove any unreacted acetic anhydride and the acetic acid by-products. The washed acetylated-CH (ACCH) obtained were then oven-dried at 60 °C for 16 h and stored in the desiccator prior to use.

2.3 Preparation of thermally and chemo-thermally modified coconut husks

The raw CH was thermally modified by the action of pyrolysis as well as chemo-thermally modified by the action of chemical activation and pyrolysis to produce un-activated and activated coconut husk-derived biochar (CHB and ACHB). The preparation of ACHB was carried out according to the method of Subha and Namasivayam [31]. The comminuted CH samples were

impregnated with zinc chloride ($ZnCl_2$) in a ratio 2:1. That is, 200 g of the sample was added to 100 g of anhydrous $ZnCl_2$ in 1 L of boiled deionized water and the mixture stirred for 1 h to form a paste, after which the remaining solution was decanted and then oven-dried at 110 °C for 1 h. The $ZnCl_2$ -impregnated CH samples were then packed inside a steel container with a tight lid. The steel container was then placed inside another larger steel container with tight lid. The inner space of this larger container was filled with sand consolidated layer by layer to the brim of the container so as to achieve a near total absence of the sample's exposure to air except for the limited oxygen already trapped in the voids of the sample. The whole setup was thereafter placed in a muffle furnace after attaining the required temperature in the furnace. The $ZnCl_2$ -impregnated CH samples were pyrolyzed at 400, 600 and 800 °C for different heating or retention time of 30, 45 and 60 min, respectively.

The activated biochar (activated coconut husk-carbon) produced from the pyrolysis or carbonization was allowed to cool to room temperature. After cooling, 100 mL of 1.0 M hydrochloric acid (HCl) was added to each of the activated CH derived-biochar (ACHB) in 500 mL beaker and the samples were left for one day so as remove or leach out excess $ZnCl_2$ present in the biochar. After that, the samples were filtered and washed thoroughly with deionized water after which 50 mL of 1.0 M NaOH was added to neutralize the acidic effects of the acid on the activated biochar. The activated CH derived-biochar (ACHB) was washed several times with deionized water until the pH of the wash water was neutral. Each of the ACHB was then filtered and oven-dried at 150 °C for 3 hours till constant weight was achieved. The ACHB were allowed to cool to room temperature and thereafter stored in an air tight containers to avoid humidity adsorption, prior to use. The ACHB produced at 400, 600 and 800 °C with retention time of 30, 45 and 60 min was respectively labelled according to its pyrolysis temperature-retention time (i.e. ACHB temperature-time) as: ACHB₄₀₀₋₃₀, ACHB₄₀₀₋₄₅, ACHB₄₀₀₋₆₀, ACHB₆₀₀₋₃₀, ACHB₆₀₀₋₄₅, ACHB₆₀₀₋₆₀, ACHB₈₀₀₋₃₀, ACHB₈₀₀₋₄₅ and ACHB₈₀₀₋₆₀. Preparation of the un-activated coconut husk derived-biochar (CHB) was carried with the same above procedure, however, without the use of $ZnCl_2$ (i.e. no chemical activation)

2.4 Characterization of sorbents

The raw CH, ACCH, ACHB₄₀₀₋₃₀, ACHB₄₀₀₋₄₅, ACHB₄₀₀₋₆₀, ACHB₆₀₀₋₃₀, ACHB₆₀₀₋₄₅, ACHB₆₀₀₋₆₀, ACHB₈₀₀₋₃₀, ACHB₈₀₀₋₄₅ and ACHB₈₀₀₋₆₀ samples were characterized for surface area using the iodine number method, volatile matter, ash content, fixed carbon, moisture content, bulk density and pH, using ASTM-D4607-94, ASTM-D1762-84 and ASTM 3172-75 standard methods [32] and functional groups using Fourier infra-red spectroscopy (FT-IR), respectively.

2.5 Determination of the degree of hydrophobicity

The degree of hydrophobicity (HD) of the sorbents were defined as the tendency of the materials to be removed from the polar aqueous phase into a non-polar liquid phase [38]. In this experiment, 1.0 g of sorbent was added into a beaker that contained 20 mL of water and was sufficiently agitated. After this, 20 mL of hexane solvent (i.e. the same volume of water) was added into the beaker and then the mixture was agitated for 3 min. Thereafter, the mixture was then left to stand for 5 min to allow for the separation of the two immiscible phases. The amount of

the sorbent transferred to the non-polar (organic) liquid phase was determined by filtration and then followed by drying and weighing. The degree of hydrophobicity of the sorbent was estimated based on Eq. (1) [38]:

$$HD(\%) = \left[\frac{W_H}{W_O} \right] \times 100 \quad (1)$$

where W_H and W_O are the weight of sorbent in hexane (g) and original weight of sorbent (g), respectively.

2.6 Remediation protocol

2.6.1 Screening of activated biochar for oil removal

The eight (8) activated biochar samples (ACHB₄₀₀₋₃₀, ACHB₄₀₀₋₄₅, ACHB₄₀₀₋₆₀, ACHB₆₀₀₋₃₀, ACHB₆₀₀₋₄₅, ACHB₆₀₀₋₆₀, ACHB₈₀₀₋₃₀, ACHB₈₀₀₋₄₅ and ACHB₈₀₀₋₆₀) prepared at different pyrolysis temperature and retention time were first screened to identify the best candidate for oil removal. One hundred (100) millilitre of the simulated marine water was placed in a 500 mL beaker and 5 g of crude oil was weighed and added. A weighed sample (0.5 g) of each ACHB was sprinkled over the crude oil-water system. The beaker was then placed on a temperature controlled water bath shaker and agitated continuously at a speed of 120 rpm for 15 min. At the end of 15 min, the wetted sorbent was taken out and allowed to drain for 5 minutes on a filter paper after which the saturated sorbent was weighed. The adsorbed water in the sample was measured using the Karl Fischer technique as well described in ASTM D1533 [39]. The quantity of sorbed oil at time, t (q_t) (i.e. oil sorption capacity) was calculated according to Eq. (2) [40] by taking into account the weight of the sorbent, the weight of the sorbent, oil and water and the weight of water:

$$q_t = \frac{M_w - (M_{wc} + M_i)}{M_i} \quad (2)$$

where, M_i is the initial mass of sorbent (g), M_w is the mass of wetted sorbent after draining (g) and M_{wc} is the mass of water content in wetted sorbent (g). All experiments were carried out in triplicate and the mean values were used for calculations. Following these preliminary sorption studies, the best performing ACHB was selected for further studies. The effects of sorption time (1- 30 min), initial oil concentration (5 – 9 g/L), temperature (15 – 35°C), sorbent dosage (0.5 – 25 g) and oil weathering number of days (3, 7 and 10 days) using the raw CH, ACCH, CHB₈₀₀₋₆₀ and ACHB₈₀₀₋₆₀ were investigated.

2.7 Data analysis

Correlations between biochar adsorption of crude oil as function of pyrolysis temperature and retention time was done using the regression analysis tool of SPSS (ver. 10) software package. Also, one-way ANOVA and Tukey Post-hoc (HSD) tests were conducted to ascertain the significant difference between the sorption capacities of the activated biochars prepared at different pyrolysis temperatures and retention times and other adsorbents used in the study.

Table 1: Characterization properties of sorbents

Parameter	Raw CH	ACHB 400 °C			ACHB 600 °C			ACHB 800 °C			CHB ₈₀₀₋₆₀	ACCH
		30	45	60	30	45	60	30	45	60		
I ₂ N (mg/g)	2.684	160.7	167.2	180.4	250.1	257.5	266.8	278.0	310.6	342.2	176.4	12.89
AC (%)	3.88	30.44	31.76	32.72	33.52	34.96	35.66	36.58	37.82	38.64	46.26	5.95
VM (%)	80.74	29.20	27.80	26.50	25.94	24.42	23.24	18.52	16.82	14.93	23.45	70.82
MC (%)	6.05	5.96	5.90	5.86	5.67	5.65	5.60	5.55	5.44	5.40	2.76	5.88
FC (%)	9.33	34.40	34.54	34.92	34.87	34.97	35.50	39.35	39.92	41.03	27.53	17.35
BD (g/cm ³)	0.084	0.324	0.310	0.284	0.266	0.242	0.226	0.210	0.197	0.183	0.743	0.137
pH	6.8	9.5	9.8	10.0	10.4	10.6	10.8	11.2	11.3	11.4	8.20	6.2

It is seen that the raw CH has a volatile matter (VM) content of 80.74% which is very high with low ash content (AC) of 3.88% and a fixed carbon (FC) of 9.33%. The BD, I₂N, and pH values for raw CH are 0.084 g/cm³, 2.684 mg/g and 6.8, respectively. However, when the raw CH was modified through acetylation reaction with acetic anhydride to produce ACCH, variations in these observed values occurred as presented for ACCH in Table 1. As it can be seen, the VM, AC, FC, BD, I₂N, and pH values of ACCH are 70.82%, 5.95%, 17.35%, 0.137 g/cm³, 12.89 mg/g and 6.2, respectively.

In addition, when the raw CH was further modified through thermo-chemical method using zinc chloride and pyrolysis at different temperature and retention time to produce activated biochar (ACHB₄₀₀₋₃₀, ACHB₄₀₀₋₄₅, ACHB₄₀₀₋₆₀, ACHB₆₀₀₋₃₀, ACHB₆₀₀₋₄₅, ACHB₆₀₀₋₆₀, ACHB₈₀₀₋₃₀, ACHB₈₀₀₋₄₅ and ACHB₈₀₀₋₆₀), there are wide variations in the physical properties in comparison with the raw CH as shown in Table 1. As it can be seen, VM, AC, FC, BD, I₂N, and pH ranged from 29.20-14.93%, 30.44–38.64%, 34.40–41.03%, 0.324-0.183 g/cm³, 160.7-342.2 mg/g, and 9.5-11.4, respectively. These values indicated that the VM and BD gradually decreased with increasing pyrolysis temperature (400–800°C) and retention time (30–60 min) while AC, FC, I₂N and pH respectively increased with increases in the pyrolysis temperature and retention time. Chen et al. [41], Angin [34] and Lee et al. [42] have reported similar observation of an increase in ash content and fixed carbon as well as a decrease in volatile matter as pyrolysis temperature increases. Suman and Gautam [43] have reported a decrease in ash content with respect to increasing temperature in the pyrolysis of coconut husk. Lee et al. [42] and Olafadehan et al. [44] have reported similar observation of a decrease in bulk density with respect to increase in pyrolysis temperature and time.

Bulk density measures the flow ability of a material. A good sorbent or adsorbent is indicated by a lower bulk density [42]. The lowest bulk density was achieved for activated biochar produced at a temperature of 800°C and retention time of 60 min (ACHB₈₀₀₋₆₀). The VM, AC, FC, BD, I₂N, and pH values of the un-activated biochar (CHB₈₀₀₋₆₀) are 23.45%, 46.26%, 27.53%, 0.743 g/cm³, 176.4 mg/g and 8.2, respectively. The pH of the sorbent constitutes a useful indicator of the nature of the functional groups present on the sorbent surface. As shown in Table 1, the pH values of raw CH and ACCH are slightly acidic while that of the un-activated and activated biochars are alkaline. The alkaline nature of the un-activated and activated biochars may be attributed to the presence of relative larger concentration of inorganic material in the form of mineral ash. Similar values of alkaline pH have been reported for carbons or biochars produced from coconut shell,

palm kernel shell, safflower seed cake, sugar beet tailings, sugarcane bagasse at high temperature [34, 42, 43, 45, 46].

The iodine number of a sorbent or material correlates with surface area and porosity or pore development [42, 44, 47]. The observed increase in iodine number with respect to increased temperature implies that the surface area and porosity of the activated biochars also increases with respect to increasing temperature and retention time. Suman and Gautam [43] have reported that the surface area and porosity of carbon produced from coconut husk increased with increase in pyrolysis temperature. Table 1 shows that high pyrolysis temperature and longer retention time would result in the release of great amount of volatile compounds from the raw material and consequently influences the iodine adsorption. The highest iodine adsorption was achieved with activated biochar produced at a pyrolysis temperature of 800°C and retention time of 60 min (ACHB₈₀₀₋₆₀ with iodine number of 342.2 mg/g). It is clearly shown in Table 1 that as the volatile matter content of the biochars decreased, the iodine adsorption of these biochars increased. Lower pyrolysis temperature and shorter retention time causes lower amount of volatile compounds to be released and thus produces biochar with underdeveloped carbon structures and reduced surface area (.). The iodine number of raw CH and ACCH are lower than the values obtained for the biochars.

3.2 FT-IR characterization

Result of the FTIR spectra carried out on raw CH, ACCH, CHB₈₀₀₋₆₀ and ACHB₈₀₀₋₆₀ are presented in Table 2. The spectra of the untreated raw CH precursor reveals the following peaks : 3560.25 – 3620.30 cm⁻¹ (-OH stretching of hydroxyl group that occur in cellulose, and N-H stretch), 2850.10 – 2965.15 cm⁻¹ (C-H asymmetric stretching of CH₂ and CH₃ of aliphatic), 1455.15 – 1652.05 cm⁻¹ (C-H deformation of CH₃, -C=C- stretching of aromatic), 1715.04 – 1840.30 cm⁻¹ (carbonyl (C=O) group of ester (ascribed to hemicellulose), 1170.11 – 1325.20 cm⁻¹ (-C-O-C stretching in cellulose, hemicellulose), (Nguyen et al., 2016).

For ACCH, the FTIR spectra revealed a peak band at 3500.11 – 3540.45 cm⁻¹ indicating the presence of OH stretching of hydroxyl group. The decrease in the OH peak intensity showed that some of the OH groups were substituted by the acetyl group and this substitution reduces the degree of hydrogen bonding [9]. The higher peak at 2900.15 – 2970.35 cm⁻¹ reveals the presence of C-H stretching of alkane (CH₂ and CH₃). This indicates an increase in the CH₂ and CH₃ (alkyl group) in ACCH and thus increase in the hydrophobicity and oleophilicity of the acetylated coconut husk.

Table 2: FT-IR spectrum analyses of raw CH, ACCH, CHB₈₀₀₋₆₀ and ACHB₈₀₀₋₆₀

Raw CH		ACCH	
Absorption Peak Number (cm ⁻¹)	Functional Groups	Absorption Peak Number (cm ⁻¹)	Functional Groups
3560.25 – 3620.30	OH (stretching), OH (non-bonding), N-H (stretching)	3500.11 – 3540.45	OH (stretching), OH (non-bonding), N-H (stretching)
2850.10 – 2965.15	C-H, CH ₂ and CH ₃ (aliphatic), COOH (carboxylic group)	2900.15 – 2970.35	C-H, CH ₂ and CH ₃ (aliphatic), COOH (carboxylic group)
1715.04 – 1840.30	C-H (aliphatic), C=C, C=O (stretching), N-H	1695.20 – 1820.40	C-H (aliphatic), C=C, C=O (stretching), N-H
1455.15 - 1652.05	C-H (deformation), N-H (bending), C=C (aromatic)	1430.23 - 1640.15	C-H (deformation), N-H (bending), C=C (aromatic)
1170.11 – 1325.20	C-O (stretching of alcohol, ether), C-N (stretching of amine)	1140.18 – 1295.25	C-O (stretching of alcohol, ether), C-N (stretching of amine)
CHB ₈₀₀₋₆₀		ACHB ₈₀₀₋₆₀	
3488.05 - 3786.60	OH (stretching), OH (non-bonding), N-H (stretching)	3446.79 - 3751.55	OH (stretching), OH (non-bonding), N-H (stretching)
1688.25 – 1810.11	C-H (alkane), C=C, C=O (stretching), N-H	1685.79 - 1799.59	C-H (aliphatic), C=C, C=O (stretching), N-H
1410.10 - 1548.60	C=C (aromatic), C-H (bending in aliphatic)	1400.32 - 1516.05	C=C (aromatic), C-H (bending in aliphatic)
1088.05 - 1190.20	C-O (stretching of alcohol, ether), C-N (stretching of amine)	1072.42 – 1147.55	C-O (stretching of alcohol, ether), C-N (stretching of amine)

This hypothesis was confirmed by the presence of carbonyl (C=O) group of ester or amides at the peak intensity of 1695.20 – 1820.40 cm⁻¹ observed in ACCH which indicates that acetylation had occurred. This observation is in good agreement with the increased degree of hydrophobicity of the raw CH from 19.4% to 65.6% after the modification. Thus, it is suggested that the increased hydrophobicity of raw CH after modification with acetic anhydride will increase the affinity of ACCH to absorb or remove more crude oil. The FTIR spectrum of ACHB₈₀₀₋₆₀ showed the presence of N-H stretch and O-H stretching (both free and H-bonded) at 3446.79 cm⁻¹ and 3751.55 cm⁻¹, confirming the presence of amine and OH groups from residual hemicellulose/cellulose. The presence of C-H stretching of aliphatic or alkane at the peak region of 2850.10-2965.15 cm⁻¹ as seen in raw CH has completely disappeared in ACHB₈₀₀₋₆₀ (i.e. peak not observed) as well as in CHB₈₀₀₋₆₀ [48]. The absence of this C-H aliphatic peak positively correlates with increased hydrophobicity in biochar. The band from 1685.79 cm⁻¹ to 1799.59 cm⁻¹ indicates the presence of carbonyl (C=O) group of ester or amides, however, a relatively higher intensity or peak (1688.25 – 1810.11 cm⁻¹) is observed in CHB₈₀₀₋₆₀. The C=C stretching of aromatic at the band region of 1400.32 cm⁻¹ to 1516.05 cm⁻¹ was observed in ACHB₈₀₀₋₆₀. While an increased band region of 1410.10 - 1548.60 cm⁻¹ was observed in CHB₈₀₀₋₆₀ as compared to ACHB₈₀₀₋₆₀. The peak observed from 1072.42–1147.55 cm⁻¹ was assigned to -C-O stretching (ascribed to cellulose and hemicellulose). However, the peaks representing C-H of aliphatic, C=C- of aromatic, C=O and OH of hydroxyl group in ACHB₈₀₀₋₆₀ and CHB₈₀₀₋₆₀ are lower as compared to the precursor which implied reduction of the functional group diversity and abundance and thus indicating increased hydrophobicity and oleophilicity of the biochar [48] which is in good agreement with the increased degree of hydrophobicity of the raw CH from 19.4% to 94.8% after the thermal and chemical

modifications. This could be the result of hemicellulose and cellulose degradation in temperature of 800 °C [25]. That is, high carbonizing or pyrolysis temperature leads to high reduction of surface functional group diversity and abundance [25, 48]. Pyrolysis of lignocellulosic biomass majorly leads to dehydroxylation or dehydrogenation reactions which results in polyaromatization of any left-over carbon. It is the presence of this polyaromaticity that contributes to the hydrophobicity and enough oleophilicity of biochar [27].

3.3 Selection of activated biochar

Figure 1 shows the oil sorption capacity of the eight types of activated biochar produced at different pyrolysis temperature of 400 – 800 °C and retention time of 30 – 60 min. At the respective temperatures of 400, 600 and 800 °C, the oil removal efficiency of each ACHB increased with increase in pyrolysis retention time (30 – 60 min). At the same pyrolysis retention time of 30-60 min, the oil sorption capacity of ACHB increased with increase in pyrolysis temperature (400 – 800 °C). Across all the activated biochars used for the treatment, the oil removal efficiency ranged from 55.2 ± 0.5 to 76.8 ± 0.5%. This suggests that a considerable percentage of oil was removed over the 15 min remediation period. Indeed, there was statistically significant difference in the oil removal efficiencies of the ACHB obtained at the different pyrolysis temperature and retention time (ANOVA: $P = 4.3 \times 10^{-20}$).

Furthermore, post hoc comparisons between the oil removal efficiencies of different pairs of ACHB (36 pairs) using Tukey's (HSD) test at 5% probability level showed that there are significant differences between the oil removal efficiencies of the different pairs with the *P-value* ranging between 0.001 and 0.018. Maximum oil removal efficiency of 76.84% was achieved with ACHB obtained at pyrolysis temperature of 800 °C and retention time of 60 min (ACHB₈₀₀₋₆₀).

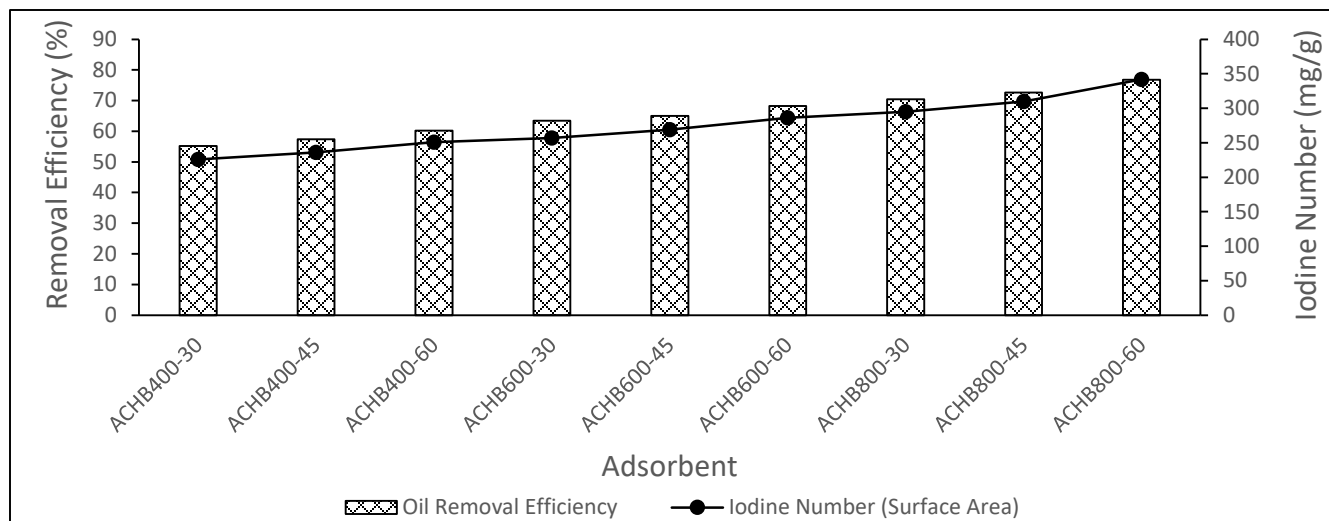


Figure 1: Oil removal efficiency of activated coconut husk derived-biochar (ACHB) produced at different temperature-time combinations

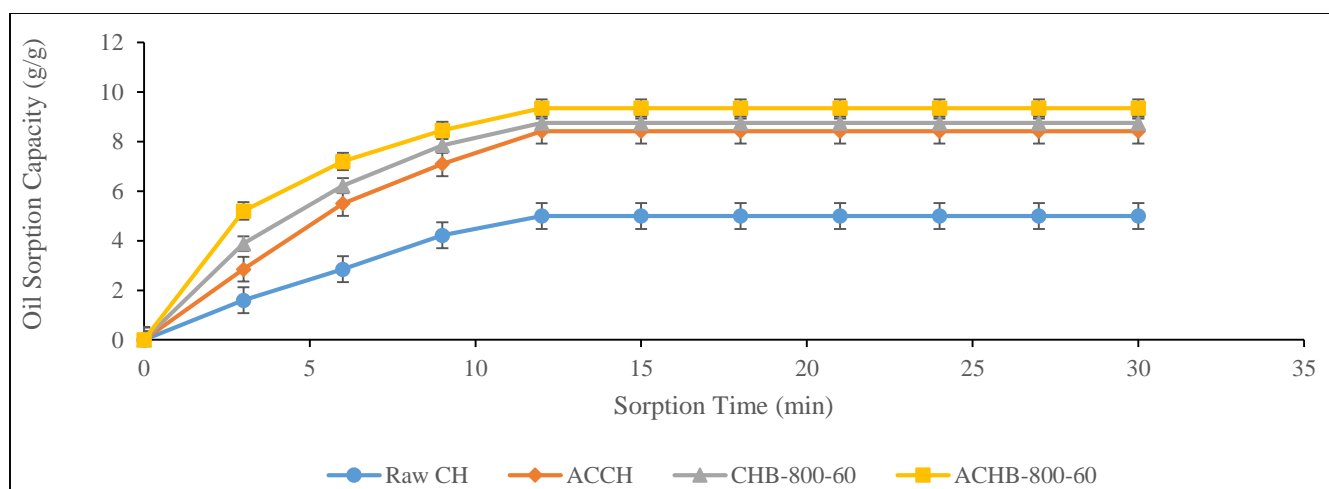


Figure 2: Effect of sorption time on oil sorption capacity of modified coconut husk (raw CH, ACCH, CHB₈₀₀₋₆₀ and ACHB₈₀₀₋₆₀)

This was followed by ACHB₆₀₀₋₆₀ and ACHB₄₀₀₋₆₀ with oil removal efficiencies of 68.2% and 60.2%, respectively. This observation suggest that oil removal efficiency of ACHB correlates positively with the pyrolysis temperature and retention time as well as with the surface area of the biochar [21, 49]. These observations are consistent with the observations reported for biochar prepared from date seed used for heavy metal removal [21] as well as for activated rubber particles used for oil removal [49]. The reason for this observation can be attributed to the effects of pyrolysis temperature on the physiochemical characteristics of the biochar including surface functional groups, structure of the pores and surface area. Sorption is a combination of adsorption and absorption. Adsorption is a surface phenomenon that has direct relationship with surface area. Thus, increasing the surface area will result in increased adsorption.

More so, surface area indirectly affects the absorption of the material to a large extent. This is because, as the surface area increases, it increases the capillaries formed and so increases the absorption [50]. Since ACHB₈₀₀₋₆₀ displayed the best

performance, it was then selected for the remaining subsequent experiments.

3.4 Effect of sorption time

The results for the effect of sorption time on oil removal is shown in Figure 2. It can be seen that the oil sorption capacity of raw CH, ACCH, CHB₈₀₀₋₆₀ and ACHB₈₀₀₋₆₀ respectively increased with the increase in sorption time. The oil sorption rapidly increase in the first 3 min and after which, it proceeded at a slow rate until the 12th minute when there was no more significant oil sorption and a maximum oil sorption capacity of 5 ± 0.13 g/g, 8.42 ± 0.01 g/g, 8.75 ± 0.02 g/g and 9.35 ± 0.01 g/g was attained by raw CH, ACCH, CHB₈₀₀₋₆₀ and ACHB₈₀₀₋₆₀, respectively. The initial high rate of oil sorption may be attributed to the presence of active sites (microscopic voids) on the sorbent surfaces which was rapidly occupied with the oil molecules while slower rate of sorption at the later stage may probably be due to the active site saturation with oil molecules where there was no more significant oil sorption and as well as the equilibrium

between the sorption and desorption processes that occurred after saturation [15, 51, 52]. Similar observations regarding the use of sorbents for oil removal have been reported [15]. The results in Figure 2 also revealed that ACHB₈₀₀₋₆₀ relatively demonstrated a higher oil sorption capacity and thus a higher oil removal efficiency than CHB₈₀₀₋₆₀ (un-activated biochar), ACCH and raw CH. This performance was closely followed by that of CHB₈₀₀₋₆₀, ACCH and raw CH, respectively. Overall, there was statistically significant difference in the sorption capacities of these sorbents (ANOVA: $P = 1.11 \times 10^{-16}$).

Post hoc comparisons using Tukey’s (HSD) test at 5% probability level were carried out to basically determine the significant difference in sorption capacity between any of the sorbents. The difference in the mean sorption capacity between pairs of sorbents were greater than the Tukey HSD value. Thus, the Tukey’s test revealed that there are significant differences in the sorption capacity between the raw CH and ACCH; between the raw CH and CHB₈₀₀₋₆₀ as well between raw CH and ACHB₈₀₀₋₆₀, respectively. It also indicates that there are significant difference in the sorption capacity between the ACCH and CHB₈₀₀₋₆₀ as well as between ACCH and ACHB₈₀₀₋₆₀ while it

further showed that there is a significant difference in the sorption capacity of CHB₈₀₀₋₆₀ and ACHB₈₀₀₋₆₀. The reason for these observations may be due to difference in the proportions of hydrophobic and hydrophilic functional groups in the sorbents [53]. In addition, the higher surface area and pore volume as indicated by the higher iodine numbers and as well as the swelling and pores filling may also have been responsible for the high oil sorption capacity and oil removal efficiency of the activated biochar [24]. Al Zubaidy [54] has reported that the oil sorption capacity of activated carbonized date palm kernel powder was higher than the un-activated carbonized date palm kernel powder while Nwadiogbu et al. [9] have reported that the oil adsorption capacity of acetylated corncob was higher than that of the raw corncob. Yusof et al. [17] have also observed and reported that esterified coconut coir had a higher oil sorption capacity than the raw coconut coir.

3.5 Effect of initial oil concentration

The changes in the oil sorption capacity and oil removal efficiency at different initial oil concentration of 5 to 9 g are illustrated in Figure 3.

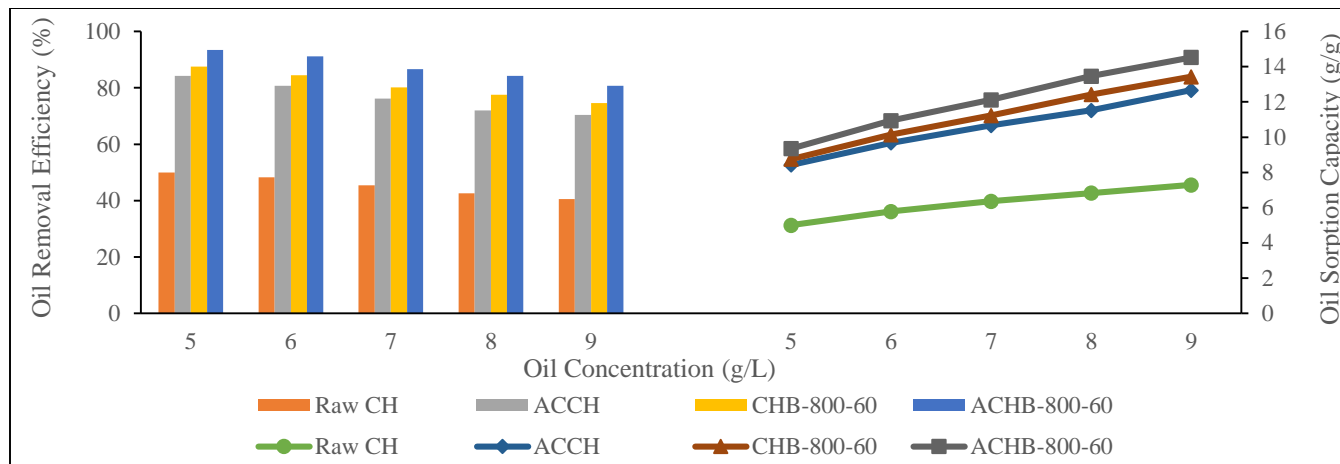


Figure 3: Effect of initial oil concentration on oil sorption capacity and oil removal efficiency of modified coconut husk

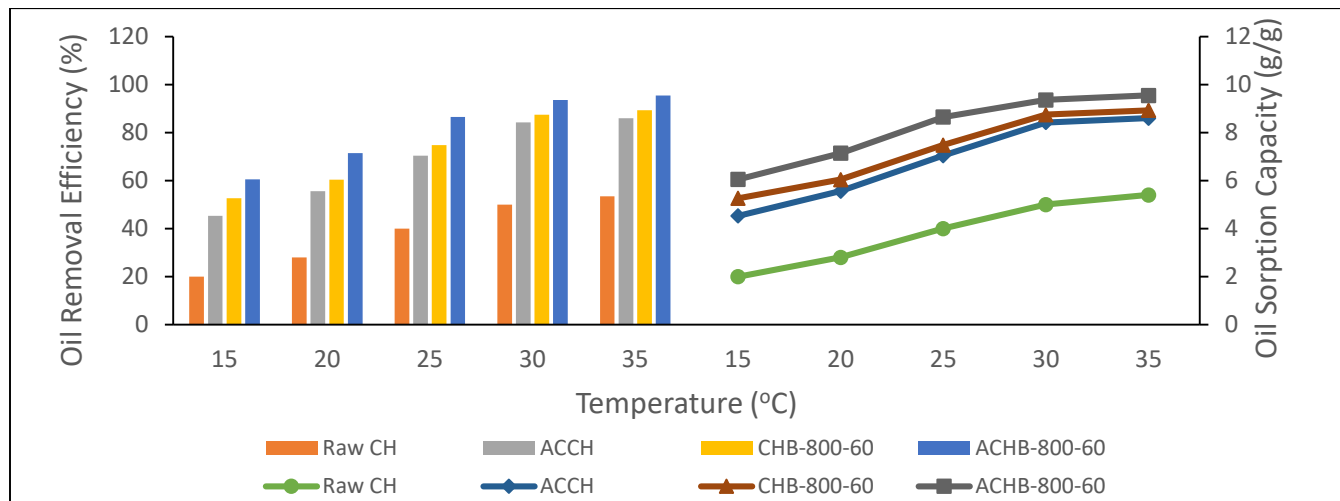


Figure 4: Effect of temperature on oil sorption capacity and oil removal efficiency of modified coconut husk

It is seen that the oil sorption capacity of raw CH, ACCH, CHB₈₀₀₋₆₀ and ACHB₈₀₀₋₆₀ respectively increased with increase in the initial oil concentration while their oil removal efficiency decreased with increase in initial oil concentration. Similar observation has been reported for esterified coconut coir in its use for oil removal from seawater with initial oil concentration of 0.05 to 0.2% mL/mL [17] as well as for bentonite/activated carbon in its use for oil removal with initial concentration of 863 to 1613 ppm [55]. Maximum oil sorption capacity of 5 g/g, 8.42 g/g, 8.75 g/g and 9.35 g/g as well as a corresponding maximum oil removal efficiency of 50%, 84.2%, 87.5% and 93.5% was attained by raw CH, ACCH, CHB₈₀₀₋₆₀ and ACHB₈₀₀₋₆₀ respectively, with the use of initial oil concentration of 5 g.

3.6 Effect of temperature

The effect of marine water temperature on the oil sorption capacity and oil removal efficiency was investigated since the temperature of marine water varies normally with seasonal change and location. Figure 4 shows the oil sorption capacity and oil removal efficiency of raw CH, ACCH, CHB₈₀₀₋₆₀ and

ACHB₈₀₀₋₆₀ at different temperature of 15 to 35 °C. The results in Figure 4 demonstrated that the oil sorption capacity and oil removal efficiency of raw CH, ACCH, CHB₈₀₀₋₆₀ and ACHB₈₀₀₋₆₀ increases with increasing temperature. A similar observation depicting an increase in the quantity of oil removed or sorbed with increase in temperature was reported by Abdelwahab [16] in his investigation of the effect of temperature on the oil sorption capacity of raw luffa fibres. Hussein et al. [18] using barley straw as well as Toyoda et al. [56] using exfoliated graphite have also reported similar observation for the adsorption of heavy crude oil. This increase in sorption may probably be due to decrease in the viscosity of the oil as temperature increases making it suitable to penetrate pores and be trapped between surface roughness until maximum oil removal is attained at 35 °C. Nevertheless, at lower temperature, the viscosity of oil is high and this may cause the oil to plug the pores and thus resulting in lower oil removal. On the other hand, decrease in oil sorption capacity with increasing temperature had been reported for the use of banana peel [13], human hair [15] and modified pomelo peel [14] in crude oil adsorption or removal.

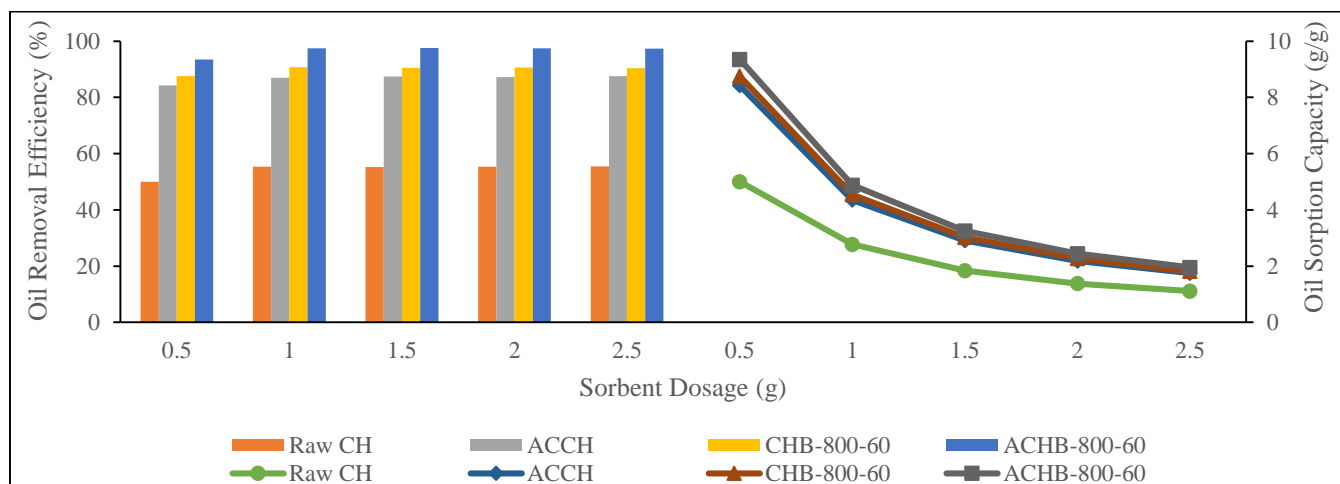


Figure 5: Effect of sorbent dosage on oil sorption capacity and oil removal efficiency of modified coconut husk

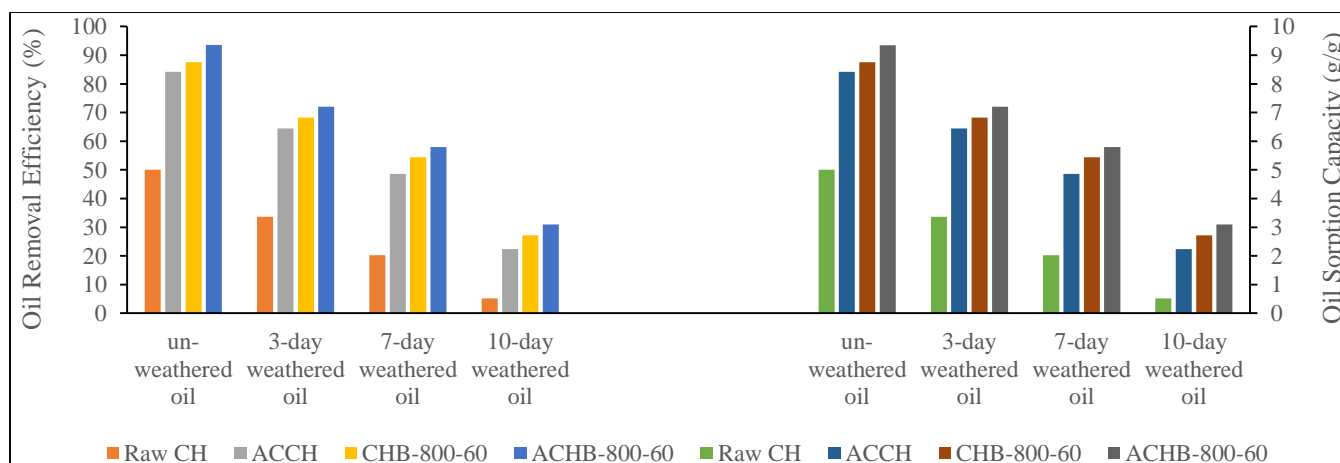


Figure 6: Effect of number of oil weathering days on oil sorption capacity and oil removal efficiency of modified coconut husk

3.7. Effect of sorbent dosage

Figure 5 shows the effect of sorbent dosage on the oil sorption capacity and oil removal efficiency. The results in Figure. 5 revealed that as the mass of the sorbents (raw CH, ACCH, CHB₈₀₀₋₆₀ and ACHB₈₀₀₋₆₀) increased from 0.5 g to 2.5 g, the oil sorption capacity decreased with a corresponding increase in oil removal efficiency. The reason for the observed decrease in oil sorption capacity may be due to the overlapping or aggregation of active adsorption sites while the observed increase in oil removal efficiency may primarily be attributed to an increased surface area and the availability of more active adsorption sites [9]. Yusof et al. [17] and Nwadiogbu et al. [9] have correspondingly reported similar observation for the use of esterified coconut coir (0.2 – 1 g) and acetylated corncob (0.5 – 2 g) in oil spill removal.

3.8 Effect of oil weathering number of days

Oil weathering is the sum of the physical and biological processes acting on oil, which change the chemical composition and physical properties, such as viscosity, over time [57]. The quantity of oil respectively adsorbed by raw CH, ACCH, CHB₈₀₀₋₆₀ and ACHB₈₀₀₋₆₀ as a function of the number of days of oil subjection to weathering effect is presented in Figure 6.

It can be seen that the oil sorption capacity as well as the oil removal efficiency relatively decreases with increase in the number of days that the oil was subjected to weathering effect. That is, the sorption capacity and removal efficiency displayed by all the sorbents (raw CH, ACCH, CHB₈₀₀₋₆₀ and ACHB₈₀₀₋₆₀) was higher for un-weathered crude oil than for the weathered oil. This observation may be attributed to increase in the viscosity of oil as the number of days for oil weathering increases. This observation is in agreement with the observation reported by Sidik et al. [38] for the use of lauric acid-modified oil palm leaves in the removal of oil not exposed to air (un-weathered oil) and the one exposed to air for 7 days (i.e. 7-days weathered oil). Nguyen and Pignatello [24] have also reported similar observation that weathered crude oil (chocolate mousse) was less absorbed by maple wood biochars and commercial biochars when compared with un-weathered crude oil. However, Hussein et al. [18] using barley straw and Alaa Eldin et al. [13] using banana peels have respectively reported increased sorption for 1-day and 7-days weathered heavy crude oil.

3.9 Adsorptive remediation (sorption) kinetic studies

Sorption kinetics helps in predicting the rate at which sorption takes place as well as assist in designing and optimising full-scale applications [15]. Sorption kinetic models of Lagergren pseudo-first-order, pseudo-second-order and intraparticle diffusion models were applied to the remediation kinetics data to analyze the rate and mechanism of crude oil sorption by raw CH, ACCH, CHB₈₀₀₋₆₀ and ACHB₈₀₀₋₆₀. The Lagergren pseudo-first-order kinetic model is expressed as given in Eq. (3) [58]:

$$\ln(q_e - q_t) = \ln q_e - kt \quad (3)$$

where q_t and q_e are the quantities of crude oil sorbed at time t (s) and at equilibrium, respectively, in g/g. k is the pseudo-first-order rate constant (min^{-1}) which can be determined from the slope of the linear plots of $\ln(q_e - q_t)$ versus t (plot not shown). The values of the constants are presented in Table 3. The results presented in Table 3 shows that the pseudo-first-order kinetic model equation

provided a good fit to the remediation kinetic data based on the high values of the regression coefficient (R^2) which were close to 1. From Table 3, it can be seen that ACHB₈₀₀₋₆₀ relatively displayed the highest rate of sorption with a higher rate constant (k) of 0.256 min^{-1} . This was closely followed by that of CHB₈₀₀₋₆₀ ($k = 0.249 \text{ min}^{-1}$), ACCH ($k = 0.231 \text{ min}^{-1}$) and raw CH ($k = 0.201 \text{ min}^{-1}$), respectively. Similarly, the pseudo-second-order kinetic model can be expressed as presented in Eq. (4) [58]:

$$\frac{t}{q_t} = \frac{1}{k_2 q_e^2} + \frac{t}{q_e} \quad (4)$$

where k_2 is the pseudo-second-order rate constant ($\text{g/g} \cdot \text{min}^{-1}$) and q_e is the theoretical equilibrium sorption capacity (g/g) both of which can be calculated from the slope and intercept of the linear plot of t/q_t versus t (plot not shown). The values of the constants are presented in Table 3. The initial sorption rate h ($\text{g g}^{-1} \text{ min}^{-1}$) was calculated from the following equation:

$$h = k_2 q_e^2 \quad (5)$$

Table 3 shows that the pseudo-second-order kinetic model equation provided a good fit to the remediation kinetics data based on the high values of the regression coefficient (R^2) which were close to 1. The R^2 values of the pseudo-second-order kinetic model equation obtained for raw CH, ACCH, CHB₈₀₀₋₆₀ and ACHB₈₀₀₋₆₀ were 0.9577, 0.9805, 0.9872 and 0.9946, respectively. The results in Table 3 revealed that ACHB₈₀₀₋₆₀ exhibited the highest initial sorption rate of oil with h value of $7.568 \text{ g/g} \cdot \text{min}$ and a faster rate of sorption with k_2 value of $0.078 \text{ g/(g} \cdot \text{min)}$ than the other sorbents. This was relatively followed by that of CHB₈₀₀₋₆₀ ($h = 4.812$; $k_2 = 0.055$), ACCH ($h = 3.797$; $k_2 = 0.044$) and raw CH ($h = 1.336$; $k_2 = 0.038$), respectively. The R^2 value of pseudo-second-order kinetic equation obtained for raw CH, ACCH and CHB₈₀₀₋₆₀ was higher than that of its pseudo-first-order kinetic equation (i.e., 0.9427, 0.9641 and 0.9807) and there exist a very good agreement between q_e (theoretical) and q_e (experimental) which suggest that the pseudo-second-order kinetic model provided a better fit to the oil remediation kinetic data of raw CH, ACCH and CHB₈₀₀₋₆₀, respectively.

Thus, the removal of oil spill by raw CH, ACCH and CHB₈₀₀₋₆₀ follows a pseudo-second-order kinetics. This is in agreement with the observation made for the use of fatty acid-modified banana trunk fiber [59], esterified coconut coir [17], human hair [15], fatty acid-modified pomelo peel [14] and lauric acid-modified oil palm leaves [38] in the removal of oil spill. While the R^2 value of pseudo-first-order kinetic equation (i.e., 0.9976) obtained for ACHB₈₀₀₋₆₀ is relatively higher than its pseudo-second-order kinetic model equation (i.e., 0.9946) and there also exist a very good agreement between q_e (theoretical) and q_e (experimental) which indicates that pseudo-first-order kinetic model provided a better fit to the kinetic data. Therefore, the removal of oil spill by ACHB₈₀₀₋₆₀ follows a pseudo-first-order kinetics. This is in agreement with the observation of Nwadiogbu et al. [9] for the use of raw and acetylated corncob. The transport of oil from the aqueous phase to the sorbent surface and then its diffusion into the interior of porous particles can be described by Weber-Morris intraparticle diffusion model.

Table 3: Pseudo first-order, pseudo second-order, intra-particle and correlation coefficients obtained for the removal of crude oil from marine water by raw CH, ACCH, CHB₈₀₀₋₆₀ and ACHB₈₀₀₋₆₀

Kinetic Model	Parameter	Raw CH	ACCH	CHB ₈₀₀₋₆₀	ACHB ₈₀₀₋₆₀
Pseudo first-order	k_1 (min ⁻¹)	0.201	0.231	0.249	0.256
	q_e (theo.) (mg/g)	5.71	9.43	9.63	9.31
	q_e (exp)	5.0	8.42	8.75	9.35
	R^2	0.9427	0.9641	0.9807	0.9974
Pseudo second-order	k_2 (g/(g.min))	0.038/0.049	0.044	0.055	0.078
	q_e (theo.) (mg/g)	5.74	9.29	9.45	9.85
	q_e (exp)	5.00	8.42	8.75	9.85
	h	1.336	3.797	4.912	7.568
	R^2	0.9577	0.9805	0.9872	0.9946
Weber-Morris Intraparticle diffusion	K_p (mg/(g min ^{0.5}))	1.45	2.43	2.59	2.74
	C	0.3514	0.2942	0.1677	0.2091
	R^2	0.9555	0.9891	0.9943	0.9946

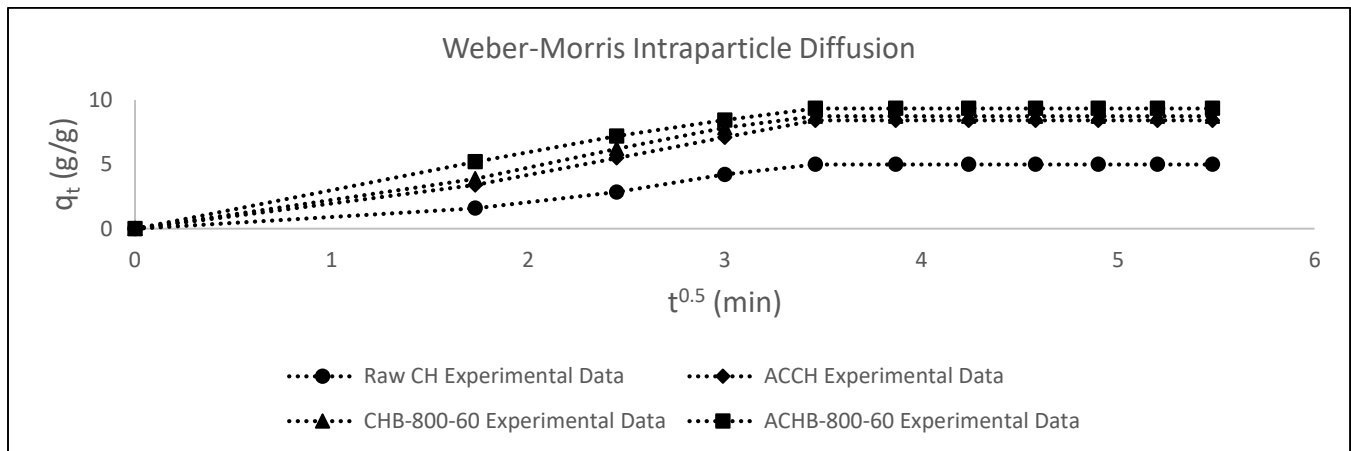


Figure 7: Application of Weber-Morris intraparticle diffusion to the sorption kinetic data of modified coconut husk

The model can be expressed as presented in Eq. (6) [58]:

$$q_t = K_d t^{0.5} + C \tag{6}$$

where K_d is the intra particle diffusion rate constant (mg/g min^{-½}) and C is the intercept. The intercept of the plot indicates the boundary layer effect and its magnitude determines the degree of the surface sorption contribution in the rate determining step. K_d can be determined from the slope of the plot of q_t vs. $t^{0.5}$. Intraparticle diffusion becomes the sole rate determining step if the plot passes through the origin [58]. In fact, the linear plots did not pass through the origin and given the multilinearity of these plots for oil removal by raw CH, ACCH and CHB₈₀₀₋₆₀ and ACHB₈₀₀₋₆₀, this suggests that oil removal occurred in three phases as shown in Figure 7.

The first steeper linear phase represents film or surface diffusion, the second linear phase represents intraparticle or pore diffusion and the third phase is final equilibrium stage where

intraparticle diffusion begins to decrease due to the extremely low sorbate concentrations in the aqueous phase [60, 61]. This observation is confirmed by the high R^2 and a non-zero intercept results obtained for raw CH, ACCH and CHB₈₀₀₋₆₀ and ACHB₈₀₀₋₆₀, respectively, as presented in Table 3. The high regression suggest the existence of an intraparticle diffusion mechanism for the sorption of crude oil by raw CH, ACCH and CHB₈₀₀₋₆₀ and ACHB₈₀₀₋₆₀. Also, the presence of the intercept C (boundary layer effect) confirmed the existence of film or surface sorption and thus indicating that intraparticle diffusion was not the only rate-controlling or determining step.

3.10 Sorption isotherms

The fundamental requirements for the design of adsorption systems are the sorption isotherms. Sorption isotherm depicts at constant temperature the equilibrium correlation or relationship that exist between the quantity of sorbate in the liquid phase and that on the surface of the sorbent [61]. A number of two, three or

four-parameter sorption isotherm models have been developed to describe equilibrium relationships in adsorption systems. In this present study, two-parameter models of Langmuir, Freundlich, and Temkin were used to analyze the equilibrium data. The linear form of Langmuir isotherm model is as given in Eq. (7):

$$\frac{1}{q_e} = \frac{1}{q_{max}b} * \frac{1}{C_e} + \frac{1}{q_{max}} \quad (7)$$

where q_{max} and b are Langmuir isotherm constants. (mg/g) is the maximum monolayer sorption capacity of the sorbent (mg/g), b (L/mg) is related to energy of adsorption, which quantitatively represents the binding affinity between the sorbent and the sorbate. The q_{max} and b can be determined from the linear plot of $1/q_e$ vs. $1/C_e$. The determined values of the Langmuir constants are presented in Table 4.

As seen in Table 4, the R^2 values are 0.9950, 0.9805, 0.9850 and 0.9868 for raw CH, ACCH, CHB₈₀₀₋₆₀ and ACHB₈₀₀₋₆₀ respectively, indicating that the Langmuir isotherm provided a good fit to the sorbents equilibrium data. It can apparently be said that when $b > 0$, sorption system is favorable [58]. In this study, b was found to be 0.286, 4.33, 1.86 and 3.74 L/mg for raw CH, ACCH, CHB₈₀₀₋₆₀ and ACHB₈₀₀₋₆₀, respectively. The value of q_{max} obtained for ACHB₈₀₀₋₆₀ (16.84 g/g) was found to be relatively higher than the other sorbents used in this study. This was closely followed by that of CHB₈₀₀₋₆₀ (16.10 g/g), ACCH (15.06 g/g) and raw CH (12.11 g/g), respectively. The q_{max} values obtained in this study are relatively comparable with the values obtained for the use of other adsorbents. Sathasivan and Mas Haris [59], Okiel et al. [55], Uzoije et al. [62], Sidik et al. [38], Asadpour et al. [63], Ifeiebuegu et al. [15], Yusof et al. [17] and Elkady et al. [64] correspondingly obtained q_{max} values of 0.149-0.476 g/g; 0.00712 g/g; 0.0014 g/g, 0.00172 g/g; 3.33 g/g, 4.226 g/g; 15.3 g/g; and 16.4 g/g for the use of fatty acid-modified banana trunk fiber, powdered activated carbon, groundnut shell-activated carbon, lauric acid-modified oil palm leaves, fatty acid-modified mangrove bark, human hair, esterified coconut coir and water hyacinth-derived Nano-activated carbon in the removal of oil from water respectively.

The Freundlich isotherm model is normally applied to non-ideal sorption on heterogeneous surfaces where binding sites are not equivalent or independent [61]. The linear form of this isotherm model can be expressed as presented in Eq. (8) [58]:

$$\ln q_e = \ln K_F + 1/n \ln C_e \quad (8)$$

where K_F and n are Freundlich constants that roughly gives an indicator of the adsorption capacity (mg/g) and the intensity of sorption. The constants can be estimated from the slope and intercept of the linear plot of $\ln q_e$ versus $\ln C_e$.

The values of the constants are presented in Table 4. The R^2 obtained for raw CH, ACCH, CHB₈₀₀₋₆₀ and ACHB₈₀₀₋₆₀ are 0.9806, 0.9896, 0.9966 and 0.9972, respectively and these values indicates that the Freundlich isotherm provided a good fit to the sorption equilibrium data. Values $1 < n < 10$ or $1/n < 1$ indicates favourable sorption [61]. In this study, the values $1/n$ for raw CH, ACCH, CHB₈₀₀₋₆₀ and ACHB₈₀₀₋₆₀ are 0.468, 0.318, 0.325 and 0.293, respectively, which indicates a favourable sorption of oil and their corresponding K_F values are 3.32, 9.11, 10.24 and 13.10 (g/g) (L/g). Smaller the values of $1/n$, the higher the affinity between sorbate and sorbent [55]. The K_F values which roughly indicates the sorption capacity revealed that ACHB₈₀₀₋₆₀ had a higher performance or sorption in comparison with the other sorbents. This was relatively followed by CHB₈₀₀₋₆₀, ACCH and raw CH, respectively. The K_F : $1/n$ values obtained in this study are relatively comparable with the values obtained for the use other adsorbents. Sathasivan and Mas Haris [59], Okiel et al. [55], Uzoije et al. [62], Sidik et al. [38], Asadpour et al. [63], Ifeiebuegu et al. [15] and Elkady et al. [64] correspondingly obtained K_F : $1/n$ values of 0.028-0.25 g/g:0.385-0.779; 10.37 mg/g:0.658; 0.0055 g/g:0.641; 1.72 mg/g: 0.719; 0.0224-0.0340 g/g: 1.477 g/g: 0.420; and 0.2751 g/g:0.926 for the use of fatty acid-modified banana trunk fiber, powdered activated carbon, groundnut shell-activated carbon, lauric acid-modified oil palm leaves, fatty acid-modified mangrove bark, human hair and water hyacinth-derived Nano-activated carbon in the removal of oil from water respectively.

Table 4: Adsorption isotherm parameters and correlation coefficients for the adsorption of crude oil by raw CH, ACCH, CHB₈₀₀₋₆₀ and ACHB₈₀₀₋₆₀

Isotherm Model	Parameter	ACHB ₈₀₀₋₆₀			
		Raw CH	ACCH	CHB ₈₀₀₋₆₀	ACHB ₈₀₀₋₆₀
Langmuir	q_{max} (g/g)	12.11	15.06	16.10	16.84
	b (L/g)	0.286	4.33	1.86	3.74
	R^2	0.9950	0.9805	0.9850	0.9868
Freundlich	K_f (g/g)(L/g)	3.32	9.11	10.24	13.10
	$1/n$	0.468	0.318	0.325	0.293
	R^2	0.9806	0.9896	0.9966	0.9972
Temkin	A (L/g)	2.379	16.08	18.51	44.49
	B	2.846	3.291	3.546	3.478
	b_T (kJ/mol)	0.8851	0.766	0.7104	0.7243
	R^2	0.9885	0.9816	0.9925	0.9972

Temkin isotherm can be represented in its linear form as [58]:

$$q_e = B \ln A + B \ln C_e \quad (9)$$

where B is related to the heat of sorption, A is the equilibrium binding constant (L/min) which corresponds to the maximum binding energy. C_e is concentration of the adsorbate at equilibrium (g/L), q_e is the amount of sorbate sorbed at equilibrium (g/g), $B = RT/b_T$ where T is the temperature in degree Kelvin and R , the ideal gas constant (8.314×10^{-3} KJ mol⁻¹ K⁻¹) and, b_T and A are constants. A and B can be determined from the linear plot of q_e vs. $\ln C_e$. The R_2 obtained for raw CH, ACCH, CHB₈₀₀₋₆₀ and ACHB₈₀₀₋₆₀ are 0.9885, 0.9816, 0.9925 and 9972, respectively and these values indicates that the Temkin isotherm also provided a good fit to the sorption equilibrium data. The values of A , B and b_T are given in Table 4. As presented in Table 4, it is seen that the constant A value for ACHB₈₀₀₋₆₀ (44.49 L/g) is higher than the values obtained for other sorbents. This shows that ACHB₈₀₀₋₆₀ had greater binding to the oil and greater oil removal than other sorbents. This was followed by that of CHB₈₀₀₋₆₀ (18.51 L/g), ACCH (16.08 L/g) and raw CH (2.379 L/g), respectively. The lower values of b_T (< 8 KJ/mol) indicate that the interaction between crude oil and each of the sorbent (raw CH, ACCH, CHB₈₀₀₋₆₀ and ACHB₈₀₀₋₆₀) was weak. Hence, the sorption process of crude oil onto raw CH, ACCH, CHB₈₀₀₋₆₀ and ACHB₈₀₀₋₆₀ can respectively be expressed as physical sorption as indicated by the value of b_T .

As shown in Table 4, it is observed that the R^2 values obtained for the application of Freundlich isotherm to the sorption equilibrium data of ACCH, CHB₈₀₀₋₆₀ and ACHB₈₀₀₋₆₀ is relatively higher than the corresponding values obtained for Langmuir and Temkin isotherms. Thus, the results revealed that the Freundlich isotherm model is more suitable for describing the sorption of crude oil by ACCH, CHB₈₀₀₋₆₀ and ACHB₈₀₀₋₆₀, respectively, than the Langmuir isotherm model. That is, the sorption of crude oil onto ACCH, CHB₈₀₀₋₆₀ and ACHB₈₀₀₋₆₀ occurred on heterogeneous binding sites with non-uniform distribution of energy. This observation is in agreement with the results reported for the use of fatty acid-modified banana trunk fibers [59], lauric acid-modified oil palm leaves [38], leaves and root of *Pistia stratiotes* [65], acetylated kapok fibers [66] and human hair [15] in the removal of oil from aqueous phase, respectively. Meanwhile, the R^2 value for Langmuir isotherm application to the sorption data of raw CH is relatively higher than the corresponding values obtained for Freundlich and Temkin isotherms. Hence, the sorption of crude oil by raw CH can better be described by the Langmuir isotherm. A similar observation has been reported for the use of raw corncob and acetylated corncob in the removal of oil [9].

4 Conclusions

Oil sorption potentials of coconut husk (raw CH) and its modified forms (ACCH, CHB₈₀₀₋₆₀ and ACHB₈₀₀₋₆₀) were evaluated and thus can be concluded that the sorption potential of coconut husk can be improved or enhanced by thermal treatment through pyrolysis and chemical treatment using acetic anhydride as agent of acetylation and zinc chloride as agent of chemical activation. The oil sorption capacities and oil removal efficiencies of raw CH, ACCH, un-activated CHB₈₀₀₋₆₀ and ACHB₈₀₀₋₆₀ were functions of sorption time, initial oil concentration, temperature,

sorbent dosage and oil weathering. The rate of oil sorption by raw CH, ACCH and un-activated CHB₈₀₀₋₆₀ respectively follows a pseudo-second order kinetics while activated CHB₈₀₀₋₆₀ follows a pseudo-first order kinetics. The sorption of oil by occurs via surface and pore diffusion mechanisms. Freundlich isotherm can be used to best describe the sorption behavior of ACCH, CHB₈₀₀₋₆₀ and ACHB₈₀₀₋₆₀ while Langmuir isotherm best describes the sorption behavior of raw CH. The degree of oil removal performance by these sorbents follows this order: ACHB₈₀₀₋₆₀ > CHB₈₀₀₋₆₀ > ACCH > raw CH. Coconut husk and its modified forms has very strong potential for utilization as effective, low-cost and eco-friendly alternative sorbents for oil spill remediation.

Acknowledgment

The authors sincerely thanked the technical staff of Thermosteel Laboratories, Warri, Delta State of Nigeria for the provision of the facilities that were used for the physical and chemical and analyses carried out on the contaminated marine water and adsorbent.

Ethical issue

Authors are aware of, and have complied with the best practice in publication ethics specifically with regard to authorship, dual submission, and manipulation of figures, competing interests and compliance with policies on research ethics. Authors have adhered to publication requirements that this submitted work is original and has not been published elsewhere in any form of language.

Competing interests

The authors wish to declare that there is no conflict of interest in this research work.

Authors' contribution

All the authors of this study have completely contributed to the data collection, data analyses and manuscript writing.

References

- [1] Doshia, B., Repoa, E., Heiskanenb, J. P. et al. (2017). Effectiveness of N,O-carboxymethyl chitosan on destabilization of Marine Diesel, Diesel and Marine-2T oil for oil spill treatment, *Carbohydrate Polymers* 167, 326–336.
- [2] Fingas, M. (2011). *Oil Spill Science and Technology: Prevention, Response, and Clean Up*, Elsevier, Burlington, MA.
- [3] Brakstad, G. O., Daling, P. S., Faksness, L. et al. (2014). Depletion and biodegradation of hydrocarbons in dispersions and emulsions of the Macondo oil generated in an oil-on-seawater mesocosm flume basin, *Marine Pollution Bulletin* 84, 125–134.
- [4] Behnood, R., Anvaripour, B., Fard, N. J. H. et al. (2013). Application of natural sorbents in crude oil adsorption, *Iran. J. Oil Gas Sci. Technol.* 2(4), 1–11.
- [5] Galblaub, O. A., Shaykhiev, I. G., Stepanova, S. V. et al. (2015). Oil spill cleanup of water surface by plant-based sorbents: Russian practices, *Process Saf. Environ. Prot.* 15, 1–15.
- [6] Alaa El-Din, G., Amer, A. A., Malsh, G. et al. (2017). Study on the use of banana peels for oil spill removal. *Alexandria Eng. J.* <http://dx.doi.org/10.1016/j.aej.2017.05.020>.
- [7] Teas, C., Kalligeros, S., Zankos, F. et al. (2001). Investigation of the effectiveness of absorbent materials in oil spill cleanup. *Desalination* 140 (3), 259–264.
- [8] Wahi, R., Chuah, L. A., Choong, T. S. Y. et al. (2013). Oil removal from 321 aqueous state by natural fibrous sorbent: an overview. *Sep.*

- Purif. Technol.* 113, 51–63. doi:<http://dx.doi.org/10.1016/j.seppur.2013.04.015>
- [9] Nwadiogbu, J. O., Ajiwe, V. I. E., and Okoye, P. A. C. (2016). Removal of crude oil from aqueous medium by sorption on hydrophobic corn cobs: Equilibrium and kinetic studies. *Journal of Taibah University for Science* 10, 56–63.
- [10] Deschamps, G., Caruel, H., Borredon, M. E. et al. (2003). Oil removal from water by selective sorption on hydrophobic cotton fibres: study of sorption properties and comparison with other cotton fibre-based sorbents. *Environ. Sci. Technol.* 37 (5), 1013–1015.
- [11] Bayat, A., Aghamiri, S. F., Moheb, A. et al. (2005). Oils spill cleanup from seawater by sorbent materials. *J. Chem. Eng. Technol.* 28, 1525–1528.
- [12] Lim, T. T. and Huang, X. (2007). Evaluation of kapok (*Ceiba pentandra* (L.) Gaertn.) as a natural hollow hydrophobic–oleophilic fibrous sorbent for oil spill cleanup. *Chemosphere* 66, 955–963.
- [13] Hussein, M., Amer, A. A., Azza El-Maghraby et al. (2009a). A comprehensive characterization of corn stalk and study of carbonized corn stalk in dye and gas oil sorption. *J. Anal. Appl. Pyrol.* 86, 360–363.
- [14] Zou, J., Liu, X., Chai, W. et al. (2014). Sorption of oil from simulated seawater by fatty acid-modified pomelo peel. *Desalination and Water Treatment*, DOI:10.1080/19443994.2014.941302
- [15] Ifelebuegu, A. O., Nguyen, T. V., Ukotije-Ikwut, P. et al. (2015). Liquid-phase sorption characteristics of human hair as a natural oil spill sorbent. *J. Environ. Chem. Eng.* 3, 938–943.
- [16] Abdelwahab, O. (2014). Assessment of raw luffa as a natural hollow oleophilic fibrous sorbent for oil spill cleanup. *Alexandria Engineering Journal* 53, 213–218.
- [17] Yusof, N. A., Mukhair, H., Abd. Malek, E. et al. (2015). Esterified coconut coir by fatty acid chloride as biosorbent in oil spill removal. *BioResources* 10 (4), 8025–8038.
- [18] Hussein, M., Amer, A. A., El-Maghraby, A. et al. (2009b). Availability of barley straw application on oil spill cleanup. *Int. J. Environ. Sci. Tech.*, 6 (1), 123–130.
- [19] Nwadiogbu, J. O., Okoye, P. A. C., Ajiwe, V. I. E. et al. (2014). Hydrophobic treatment of corn cob by acetylation: kinetic and thermodynamic studies. *J. Environ. Chem. Eng.* 2, 1699–1705
- [20] Sun, X. F., Sun, R. C., and Sun, J. X. (2004). Acetylation of sugarcane bagasse using NBS as a catalyst under mild reaction conditions for the production of oil sorption-active materials. *Bioresource Technol.* 95, 343–350.
- [21] Mahdi, Z., Yu, Q., and El Hanandeh, A. (2018). Investigation of the kinetics and mechanisms of nickel and copper ions adsorption from aqueous solutions by date seed derived biochar, *Environ. Chem. Eng.* 6, 1171–1181.
- [22] El Hanandeh, A., Abu-Zuryk, R. A., Hamdneh, I. et al. (2016). Characterization of biochar prepared from slow pyrolysis of Jordanian olive oil processing solid waste and adsorption efficiency of Hg^{2+} ions in aqueous solutions. *Water Sci. Technol.* 74, 1899–1910.
- [23] Li, B., Yang, L., Wang, C. Q. et al. (2017). Adsorption of Cd (II) from aqueous solutions by rape straw biochar derived from different modification processes. *Chemosphere* 175, 332–340.
- [24] Nguyen, H. N. and Pignatello, J. J. (2013). Laboratory tests of biochars as adsorbents for use in recovery or containment of marine crude oil spills. *Environ. Eng. Sci.* 30 (7), 374–380.
- [25] Nguyen, T. H., Cat, L. V., Anh, P. V. et al. (2016). Research on oil adsorption capacity of carbonized material derived from agricultural by-product (corn cob, corn stalk, rice husk) using in oily wastewater treatment. *VNU J. Sci.: Nat. Sci. Technol.* 32 (3), 105–111
- [26] Silvani, L., Vrchotova, B., Kastanek, P. et al. (2017). Characterizing biochar as alternative sorbent for oil spill remediation. *Sci. Rep.* 7, 43912.
- [27] Kandaneli, R., Meesala, L., Kumar, J. et al. (2018). Cost effective and practically viable oil spillage mitigation: Comprehensive study with biochar. *Marine Pollution Bulletin* 128, 32–40.
- [28] Camilli, R., Reddy, C. M., Yoerger, D. R. et al. (2010). Tracking hydrocarbon plume transport and biodegradation at Deep water horizon. *Science* 330, 201–204.
- [29] Reddy, C. M., Arey, J. S., Seewald, J. S. et al. (2012). Composition and fate of gas and oil released to the water column during the Deep water horizon oil spill. *Proc. Natl. Acad. Sci.* 109, 20229–20234.
- [30] Kester, D. R., Duedall, I. W., Connors, D. N. et al. (1967). Preparation of artificial seawater. *Limnol. Oceanogr.* 12 (1), 176–179
- [31] Subha, R. and Namasivayam, C. (2010). ZnCl₂-Modified activated carbon from biomass coir pith for the removal of 2-chlorophenol by adsorption process. *Bioremediation J.* 14 (1), 1–9, DOI: 10.1080/10889860903455360
- [32] Demirbas, A. (2004). Combustion characteristics of different biomass fuels. *Prog. Energy Combust. Sci.* 30, 219–230.
- [33] Ilaboya, L. R., Oti, E. O., Ekoh, G. O. et al. (2013). Performance of Activated carbon from cassava peels for the treatment of effluent wastewater. *Iranical J. Energy and Environ.* 4(4), 361–375.
- [34] Angin, D. (2013). Effect of pyrolysis temperature and heating rate on biochar obtained from pyrolysis of safflower seed press cake. *Bioresour. Technol.* 128, 593–597.
- [35] ASTM D2867-09 (2009). "Standard Test Methods for Moisture in Activated Carbon", ASTM International, West Conshohocken, PA, 10.1520/D2867-09
- [36] ASTM D2854-70 (2009). "Standard Test Method for Apparent Density of Activated Carbon", ASTM International, West Conshohocken, PA. DOI: 10.1520/D2854-70.
- [37] Egbomwan, B. O. and Ezech, C. P. (2013). Comparative study of the physiochemical and structural properties of brown and green coconut fibre as low-cost adsorbents. *JORIND* 11(1), 59–66.
- [38] Sidik, S. M., Jalil, A. A., Triwahyono, S. et al. (2012). Modified oil palm leaves adsorbent with enhanced hydrophobicity for crude oil removal. *Chem. Eng. J.* 203, 9–18.
- [39] ASTM D1533-00 (2005). Annual Book of ASTM Standards, vol. 10.3, American Society of Testing and Materials, Philadelphia.
- [40] Al Zubaidy, I. A. H., Zaffar, U., Chowdhury, N. et al. (2015). Adsorption study of bio-degradable natural sorbents for remediation of water from crude oil in: *6th International Conference on Environmental Science and Technology Volume 84 of IPCBEE (2015)* DOI: 10.7763/IPCBEE.2015.V84.24
- [41] Chen, Y., Yang, H., Wang, X. et al. (2012). Biomass-based pyrolytic polygeneration system on cotton stalk pyrolysis: influence of temperature. *Bioresour. Technol.* 107, 411–418.
- [42] Lee, C. L., H'ng, P. S., Paridah, T. et al. (2017). Effect of reaction time and temperature on the properties of carbon black made from palm kernel and coconut shell. *Asian J. Sci. Res.* 10, 24–33.
- [43] Suman, S. and Gautam, S. (2017). Pyrolysis of coconut husk biomass: Analysis of its biochar properties, Energy Sources, Part A: Recovery, Utilization, and Environmental Effects. DOI: 10.1080/15567036.2016.1263252
- [44] Olafadehan, O. A., Jinadu, O. W., Salami, L. et al. (2012). Treatment of brewery wastewater effluent using activated carbon prepared from coconut shell. *Int. J. Appl. Sci. Technol.* 12 (1), 165–178.
- [45] Yao, Y., Gao, B., Inyang, M. et al. (2011). Biochar derived from anaerobically digested sugar beet tailings: characterization and phosphate removal potential. *Bioresour. Technol.* 102, 6273–6278.
- [46] Inyang, M., Gao, B., Pullammanappallil, P. et al. (2010). Biochar from anaerobically digested sugarcane bagasse. *Bioresour. Technol.* 101, 8868–8872.
- [47] Keller, G. E., Anderson, R. A., and Yon, C. M. (1987). Adsorption In: *Handbook of Separation Process Technology*, edited by Rousseau R. W., Wiley-Interscience, New York.
- [48] Gray, M., Johnson, M. G., Dragila, M. I. et al. (2014). Water uptake in biochars: the roles of porosity and hydrophobicity. *Biomass and Bioenergy* 61, 196 - 205.
- [49] Aisien, F. A. and Aisien, E. T. (2012). Application of activated recycled rubber from used tyres in oil spill cleanup. *Turkish J. Eng. Env. Sci.* 36, 171 – 177.

- [50] Hussein, M., Amer, A. A. and Sawsan, Is. Ib. (2009c). Oil spill sorption using carbonized pith bagasse: application of carbonized pith bagasses as loose fibres. *Global Nest J.* 11 (4), 440-448.
- [51] Rengasamy, R. S., Das, D., and Karan, C. P. (2011). Study of oil sorption behavior of filled and structured fiber assemblies made from polypropylene, kapok and milkweed fibers. *J. Hazard. Mater.* 186 (1), 526–532. doi:http://dx.doi.org/10.1016/j.jhazmat.2010.11.031. 21146290.
- [52] Lin, J., Shang, Y., Ding, B. et al. (2012). Nanoporous polystyrene fibers for oil spill cleanup. *Mar. Pollut. Bull.* 64 (2), 347–352. doi:http://dx.doi.org/10.1016/j.marpolbul.2011.11.002. 22136762.
- [53] Novak, J. M., Busscher, W. J., Watts, D. W. et al. (2012). Biochars impact on soil-moisture storage in an ultisol and two aridisols. *Soil Sci.* 177(5), 310-320.
- [54] Al Zubaidy, I. A. (2012). Effect of activation of date palm kernel powder on the remediation process of oil polluted water. *Int. J. Environ. Poll. Remed.* 1 (1), 54-59.
- [55] Okiel, K., El-Sayed, M., and El-Kady, M. Y. (2011). Treatment of oil–water emulsions by adsorption onto activated carbon, bentonite and deposited carbon. *Egyptian J. Petrol.* 20, 9–15.
- [56] Toyoda, M., Moriya, K., Aizawa, J. et al. (2000). Sorption and recovery of heavy oils by using exfoliated graphite Part I" Maximum sorption capacity. *Desalination* 128, 205-211.
- [57] Soloviev, A. V., Haus, B. K., McGauley, M. G. et al. (2016). Surface dynamics of crude and weathered oil in the presence of dispersants: Laboratory experiment and numerical simulation. *J. Geophys. Res. Oceans* 121, 3502–3516.
- [58] Agarry, S. E. (2019). Anthracene bioadsorption from simulated wastewater by chemically-treated unripe plantain peel bioadsorbent: Batch kinetics and isothermal modeling studies, *Polycyclic Aromatic Compounds* 39 (1), 23-43. DOI:10.1080/10406638.2016.1255650.
- [59] Sathasivam, K., and Haris, M. R. H. M. (2010) Adsorption kinetics and capacity of fatty acid-modified banana trunk fibers for oil in water. *Water, Air, Soil Pollut.* 213, 413–423.
- [60] Koyuncu, H. (2008). Adsorption kinetics of 3-hydroxybenzaldehyde on native and activated bentonite. *Appl. Clay Sci.* 38, 279–287.
- [61] Agarry, S. E. and Ogunleye, O. O. (2014). Chemically treated kola nut pod as low-cost natural adsorbent for the removal of 2,4-dinitrophenol from synthetic wastewater: batch equilibrium, kinetic and thermodynamic modeling studies. *Turkish J. Eng. Environ. Sci.* 38, 11- 40.
- [62] Uzoije, A. P., Onunkwo-A, A., and Egwuonwu, N. (2011). Crude oil sorption onto groundnut shell activated carbon: kinetic and isotherm studies. *Res. J. Environ. Earth Sci.* 3(5), 555-563.
- [63] Asadpour, R., Bin Sapari, N., Isa, M. H. (2014). Enhancing the hydrophobicity of mangrove bark by esterification for oil adsorption. *Water Sci. & Technol.* 70 (7), 1220-1228.
- [64] Elkady, M. F., Mohamed Hussien, and Reham Abou-rady (2015). Equilibrium and kinetics behavior of oil spill process onto synthesized Nano-activated carbon. *Amer. J. Appl. Chem.* 3 (3-1), 22-30.
- [65] Sánchez-Galván, G., Mercado, F. J., and Olguín, E. J. (2013). Leaves and roots of *Pistia stratiotes* as sorbent materials for the removal of crude oil from saline solutions. *Water Air Soil Pollut.* 224 (2), 1–12. doi:http://dx.doi.org/10.1007/s11270-012-4091421-0.
- [66] Wang, J., Zheng, Y., and Wang, A. (2013). Investigation of acetylated kapok fibers on the sorption of oil in water. *J. Environ. Sci.* 25 (2), 246–253. doi: 411 http://dx.doi.org/10.1016/S1001-0742(12)60031-X. 23596942